Electronic Supplementary Material (ESI) for ChemComm.

Supplementary Information

Iodine-Doped Covalent Organic Frameworks with Coaxially Stacked Cruciform Anthracenes for High Hall Mobility

Yunyang Zhu,[a] Weijun Weng,[a] Ting Zhou,[a] Zheng Lin,[a] Ning Ding,[a] Phornphimon Maitarad,[b] Changchun Wanga and Jia Guo*[a]

[a]*State Key Laboratory of Molecular Engineering of Polymers, Department of Macromolecular Science, Fudan University, Shanghai 200438, P. R. China.*
[b]*Research Center of Nano Science and Technology, Department of Chemistry, College of Science, Shanghai University, Shanghai 200444, P. R. China.*
**E-mail: guojia@fudan.edu.cn*

1. Materials and Methods

1.1 Materials

4,4,5,5-tetramethyl-2-[10-(tetramethyl-1,3,2-dioxaborolan-2-yl)anthracen-9-yl]-1,3,2-dioxaborolane was purchased from TCI chemicals. 5-bromobenzene-1,3-dicarbaldehyde was purchased from Bide pharmatech. $Pd(PPh_3)_4$ was purchased from Energy Chemical. Iodine was purchased from Shanghai Macklin Biochemical Co., Ltd. K_2CO_3 and all the solvents were purchased from Sinopharm Chemical Reagent Co., Ltd.

1.2 Characterizations

FT-IR spectra were recorded on a Nicolet 6700 (Thermofisher, USA) Fourier transformation infrared spectrometer. UV-vis-NIR absorption spectra were collected on a Lambda 750 (Perkin-Elmer, USA) UV-vis-NIR spectrophotometer. Liquid ^{1}H NMR and ^{13}C NMR spectra were recorded on a Varian Mercury plus 400 MHz spectrophotometer at 298 K. Solid-state ^{13}C cross-polarization magic-angle-spinning (CP/MAS) NMR spectrum was collected on a Bruker 400M spectrophotometer. MALDI-TOF mass spectrum was collected on a 5800 (AB SCIEX, USA) MALDI-TOF mass spectrometer. Elemental Analysis was performed on an Elementar Varioel-III elementary analyzer. TGA experiment was performed on a Pyris 1 (PE, USA) Thermogravimetric analyzer. Powder X-ray diffraction (PXRD) spectra were collected on an X-ray diffraction spectrometer (Bruker D8 Advance, Germany) with Cu Kα radiation at $\lambda = 0.154$ nm operating at 40 kV and 40 mA. N_2 sorption isotherms were collected by a TriStar II 3020 volumetric adsorption analyzer (Micromeritics, USA) at 77K. Pore size distribution was calculated by data collected by an ASAP 2460 volumetric adsorption analyzer (Micromeritics, USA) at 77K. The samples were degassed at 120^{o}C for 12 h under vacuum condition before measurement. FESEM image was taken using an Ultra 55 (Zeiss, Germany) field emission scanning electron microscope. The ESR experiments were performed on a Bruker a300 ESR

spectrometer. The Mott-Schottky plots and I-V curves were collected on a CHI-760 electrochemical workstation. Hall Measurements were finished on a PPMS-9 Hall effect tester. Electroconductivity was measured on a ST2263 double testing digital four-probe tester. Sample of 40 mg was transferred to a pressing die and pressed under the pressure of 28 MPa for 10 min. The sample was shaped as a cylindrical pellet with the diameter of 1.3 cm and thickness of 0.2 mm. The pellets were used to perform conductivity tests, Hall measurements and I-V tests afterwards.

1.3 Synthesis

1.3.1 Synthesis of 9,10-bis(3,5-diformyl-phenyl)-anthracene (BDFPA) 1

A suspension of 4,4,5,5-tetramethyl-2-[10-(tetramethyl-1,3,2-dioxaborolan-2-yl)anthracen-9-yl]-1,3,2-dioxaborolane (2.1512 g, 5mmol), 5-bromobenzene-1,3-dicarbaldehyde (2.5000 g, 11.80 mmol, 2.36 equiv.), K_2CO_3 (1.3182 g, 5 mmol), $Pd(PPh_3)_4$ (500 mg, 0.43 mmol) in toluene/H_2O (4:1, 150 mL) was added into a 250 mL Schlenk flask and degassed by three freeze-pump-thaw cycles. Then the mixture was stirred at 95^{o}C for 24 h. Liquid in the mixture was removed by rotary evaporation. The remnant solid was dispersed in CH_2Cl_2 (180 mL) and washed by brine (500 mL×4). The obtained yellow liquid was dried by anhydrous Na_2SO_4. After filtration, the crude was concentrated by rotary evaporation and purified by column chromatography (ethyl acetate: petroleum ether =1:8) to give **1** (228 mg, 10% yield) as yellow solid. ^{1}H NMR (400 MHz, $CDCl_3$, PPM): δ 7.42(dd, 4H, J=3.35 Hz), 7.55(dd, 4H, J=3.35 Hz), 8.29(s, 4H), 8.62(s, 2H), 10.26(s, 4H); ^{13}C NMR (400 MHz, $CDCl_3$, PPM): δ 126.37, 126.38, 129.80, 130.14, 134.91,137.56,137.60, 141.30, 191.05; MALDI-TOF MS: m/z calculated: 442.12 (M),443.12 (M+H); found: 442.18 (M), 443.18 (M+H).

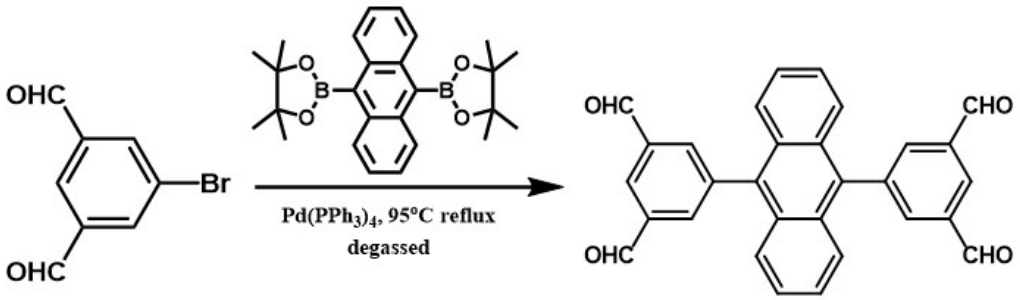

Scheme S1. Synthesis of compound **1**.

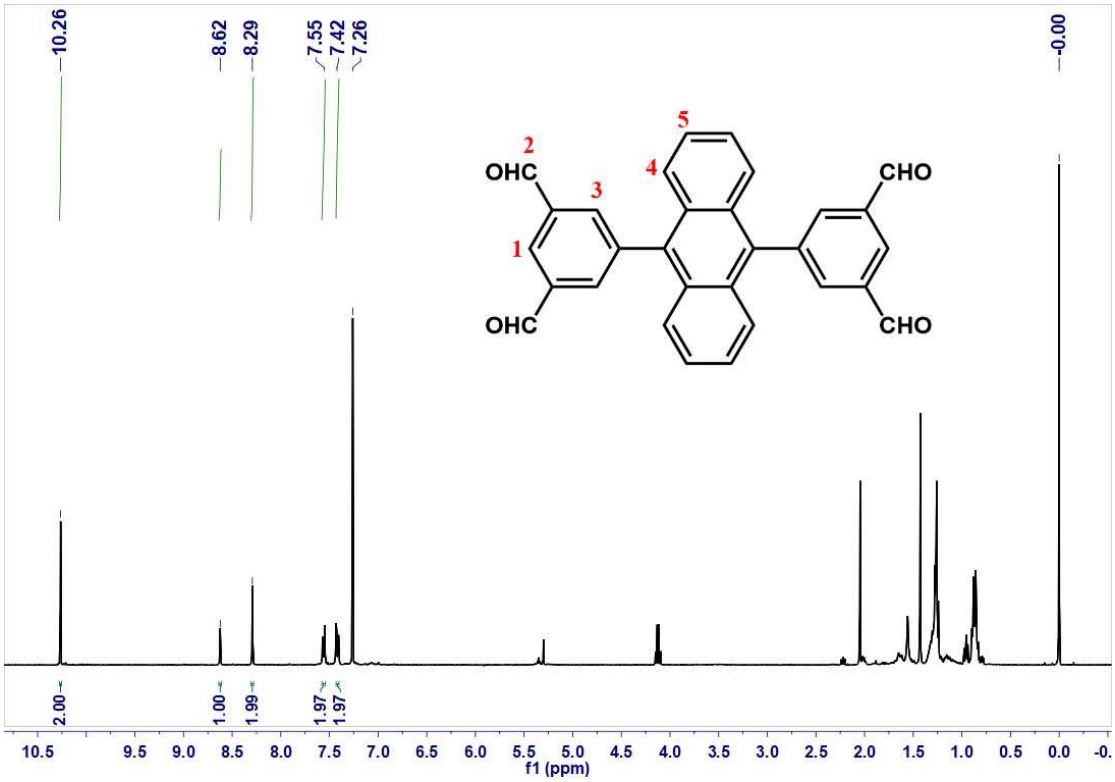

Figure S1. ^{1}H NMR spectrum of compound **1**.

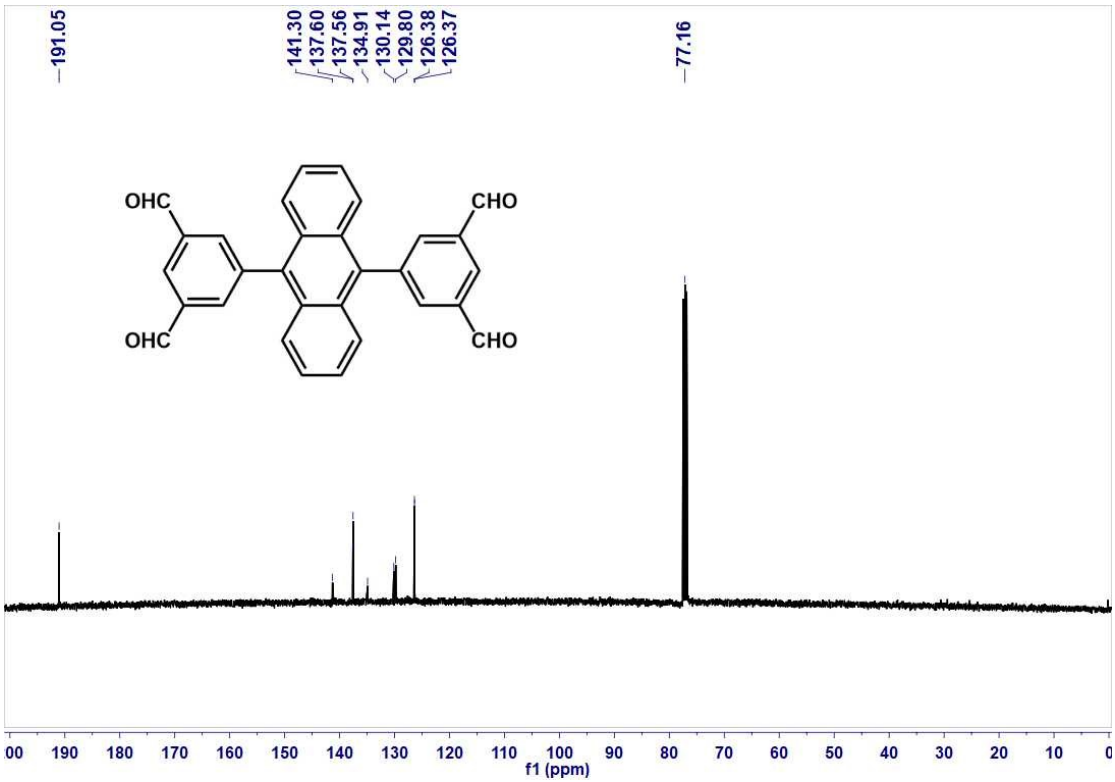

Figure S2. ^{13}C NMR spectrum of compound **1**.

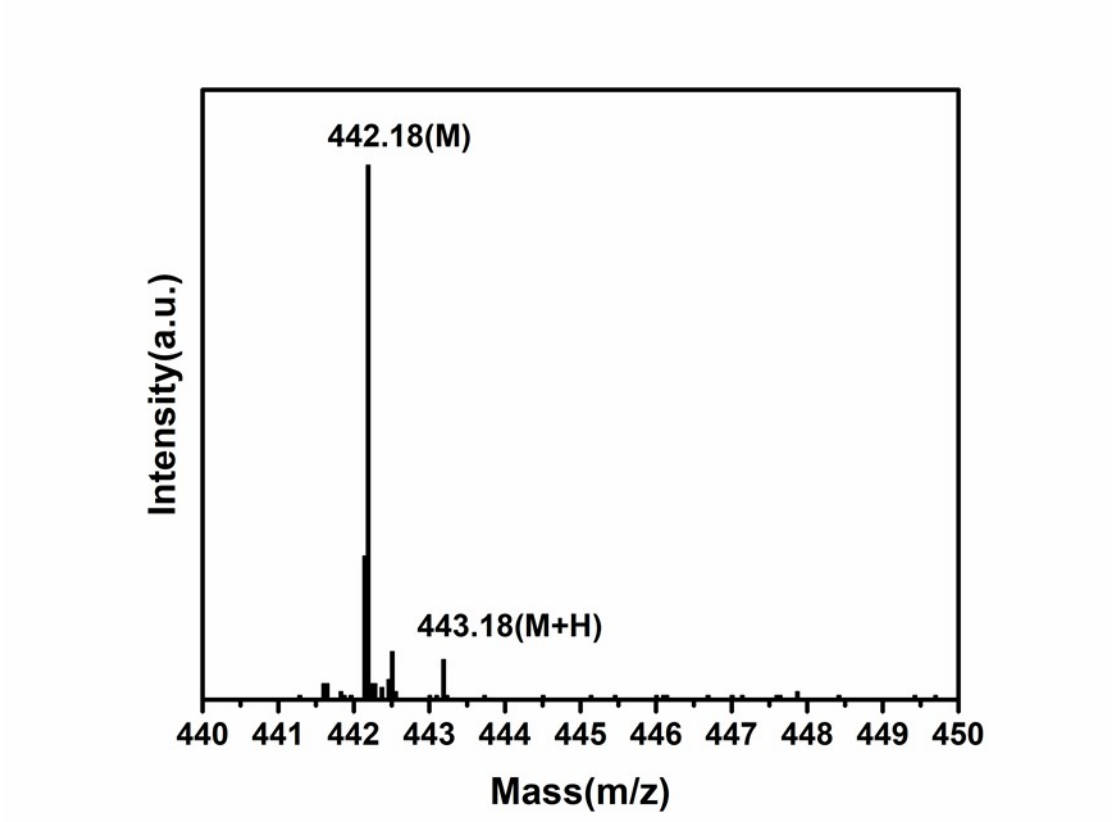

Figure S3. MALDI-TOF MS of compound **1**.

1.3.2 Synthesis of AnPD-COF

BDFPA (20.46mg, 0.0463mmol), p-phenylenediamine (10mg, 0.0926mmol) were charged into a Pyrex tube (10 cm×1 cm) and a mixture of 0.5 mL mesitylene and 0.5 mL ethanol. Then 0.1 mL 6M acetic acid (HOAc) aqueous solution was added. After sonication for 10 min, the reaction solution was subjected to three freeze-pump-thaw cycles and the Pyrex tube was sealed off. The reaction proceeded at 120^{o}C for 3 days. After cooled to room temperature, the solids were collected by filtration and washed by water, ethanol and THF. The monomers and oligomers were further removed by Soxhlet extraction with THF for 24 h. The obtained solids were dried at 40^{o}C in vacuum for 48 h, giving a yield of 82%.

1.3.3 Synthesis of Poly-AnPD

BDFPA(20.46mg, 0.0463mmol), p-phenylenediamine (10mg, 0.0926mmol) were charged into a Pyrex tube (10 cm×1cm) and mixed with 0.5 mL mesitylene and 0.5 mL dioxane. Then 0.1 mL 6M acetic acid (HOAc) aqueous solution was added. After sonication for 10 min, the reaction solution was subjected to three freeze-pump-thaw cycles and the Pyrex tube was sealed off. The reaction proceeded at 120^{o}C for 3 days. After cooled to room temperature, the solids were collected by filtration, washed by water, ethanol and THF, and extracted by Soxhlet with THF for 24 h. The obtained solids were dried at 40^{o}C under vacuum for 48 h, giving a yield of 90%.

1.3.4 Synthesis of TFB-Bp-COF

The synthesis of TFB-Bp-COF is following the method in a reported article[1]. 1,3,5-triformylbenzene (TFB, 24.3mg, 0.15 mmol), benzidine (Bp for biphenyl, 41.5mg, 0.225mmol) were charged into a Pyrex tube (10 cm×1cm) and mixed with 0.75mL mesitylene and 0.75mL dioxane. Then 0.15 mL 6M acetic acid (HOAc) aqueous solution was added. After sonication for 10 min, the reaction solution was subjected to three freeze-pump-thaw cycles and the Pyrex tube was sealed off. The reaction proceeded at 120^{o}C for 3 days. After cooled to room temperature, the solids were

collected by filtration, washed by water, ethanol and THF, and extracted by Soxhlet with THF for 24 h. The obtained solids were dried at 40°C under vacuum for 48 h, giving a yield of 85%.

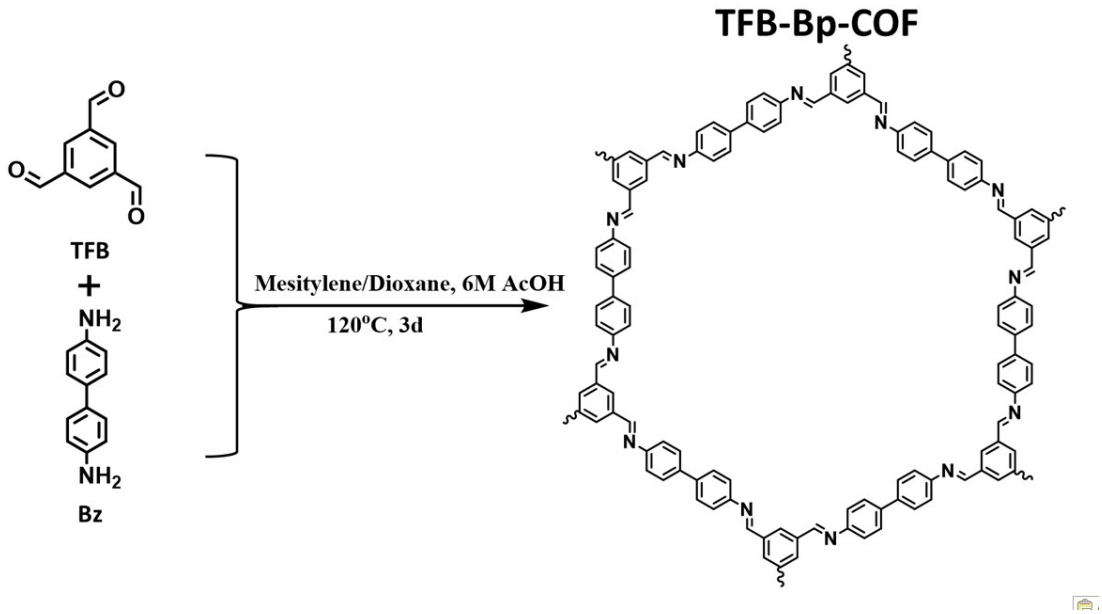

Scheme S2. Synthesis of TFB-Bp-COF.

1.3.5 Iodine doping of samples.

30 mg of pristine sample in a small bottle was placed inside a larger jar containing 2 g of iodine. The jar was heated to 50°C and the doping was monitored by the change of sample weight. After 48 h, there was negligible change henceforth and the doping was over.

1.3.6 Iodine removal of AnPD-COF.

20mg of iodine-doped AnPD-COF was dispersed in EtOH. The COF powder was washed with excessive EtOH and collected by filtration. The obtained solids were dried at 40°C in vacuum for 48 h.

1.4 Structural Modelling and Refinement

Stacking structures were built and fully optimized with the QEq charge equation by the Forcite Module of Material Studio Software. And the Pawley refinement of the experimental PXRD pattern was calculated using the Reflex Module.

1.5 Calculation of Ionization Potentials

The DFT calculations were performed by Gaussian 16 package[2] on the level of M062X/def2TZVP[3], involving the D3 version of Grimme's dispersion correction[4]. The structural models were cutout from the crystal structure of the reported literature[1] and this work for further optimization. The ionization potentials were calculated by the following equation[5]:

Vertical Ionization Potential = Energy of Cation Species – Energy of Neutral Species

where cation species and neutral species were both optimized in the neutral state.

2. Figures and Tables

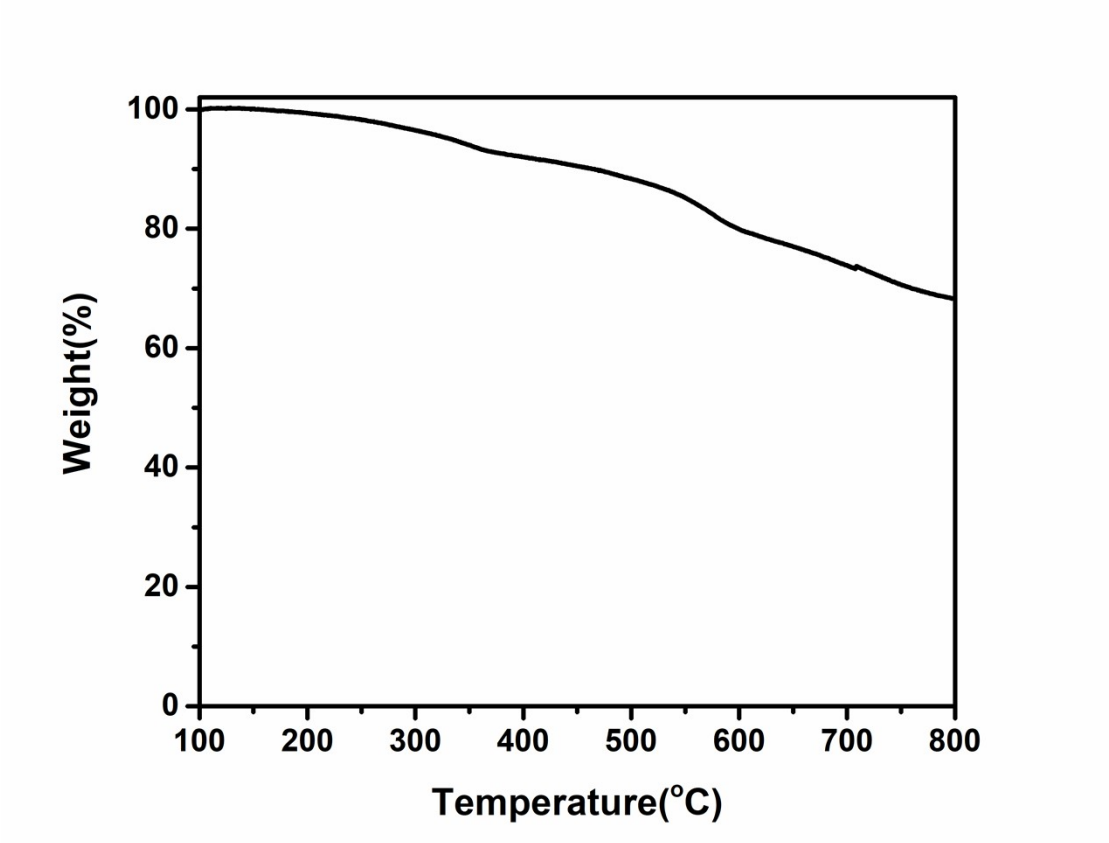

Figure S4. TGA curve of AnPD-COF.

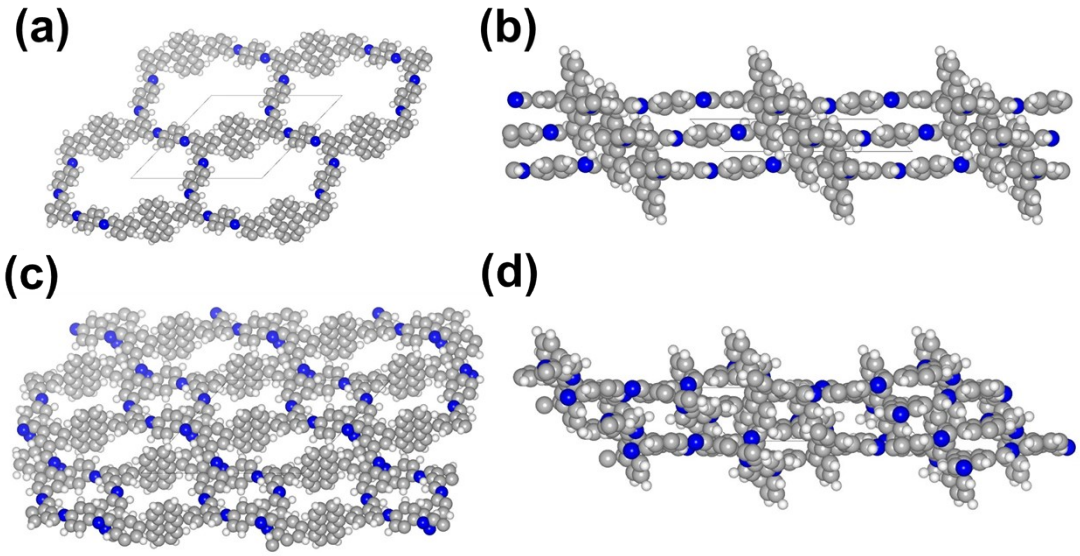

Figure S5. Models of AnPD-COF with two kinds of stacking modes. (a) top and (b) side view of AA stacking mode. (c) top and (d) side view of AB stacking mode. carbon: gray; Nitrogen: blue; Hydrogen: white.

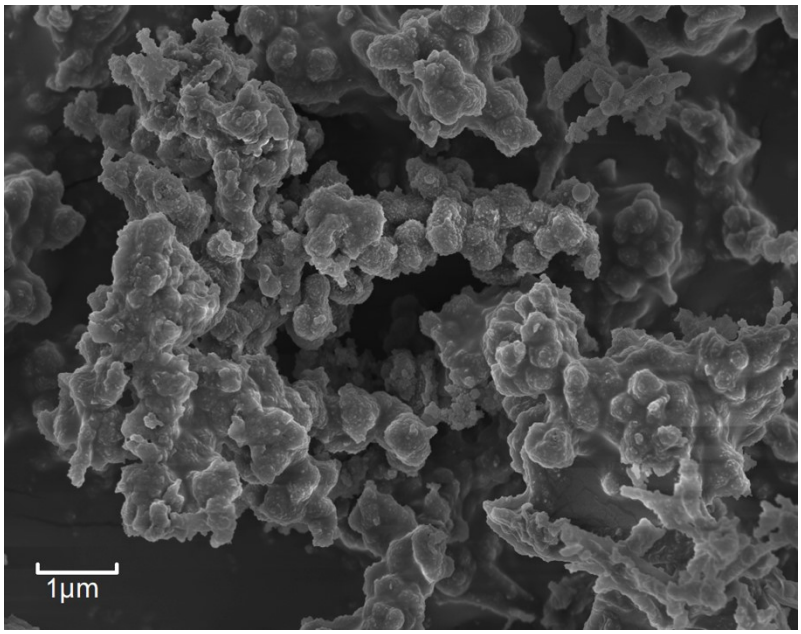

Figure S6. FE SEM image of AnPD-COF.

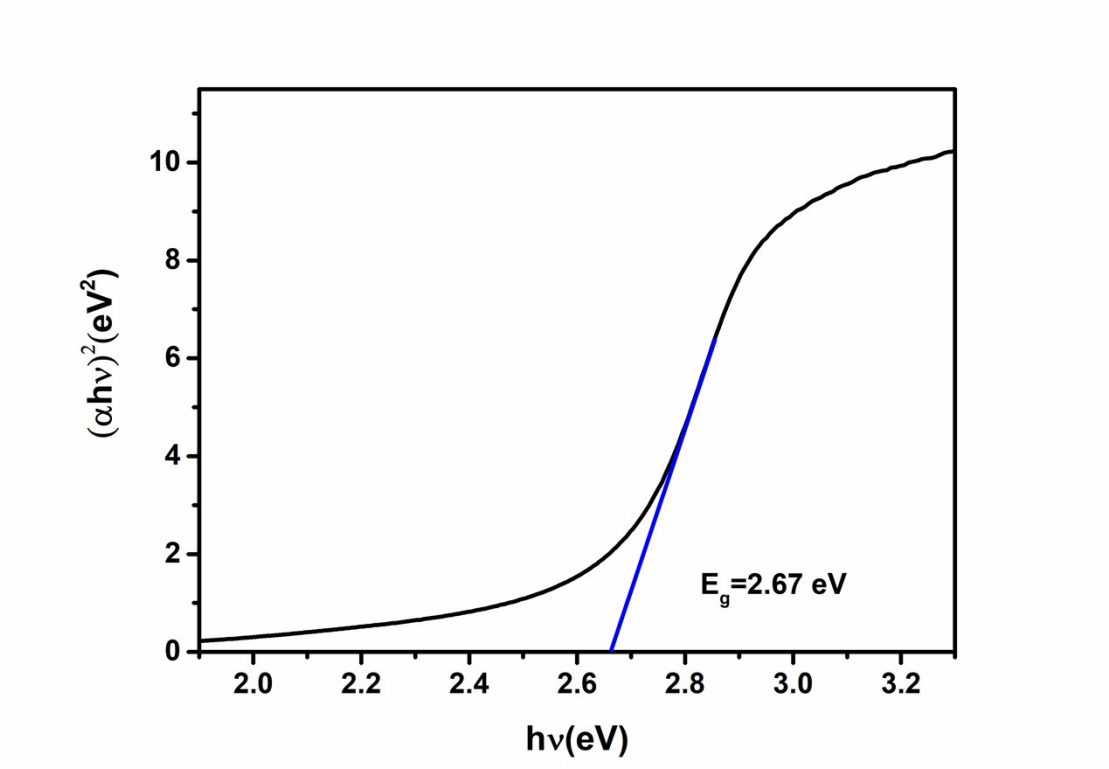

Figure S7. Tauc plot of AnPD-COF.

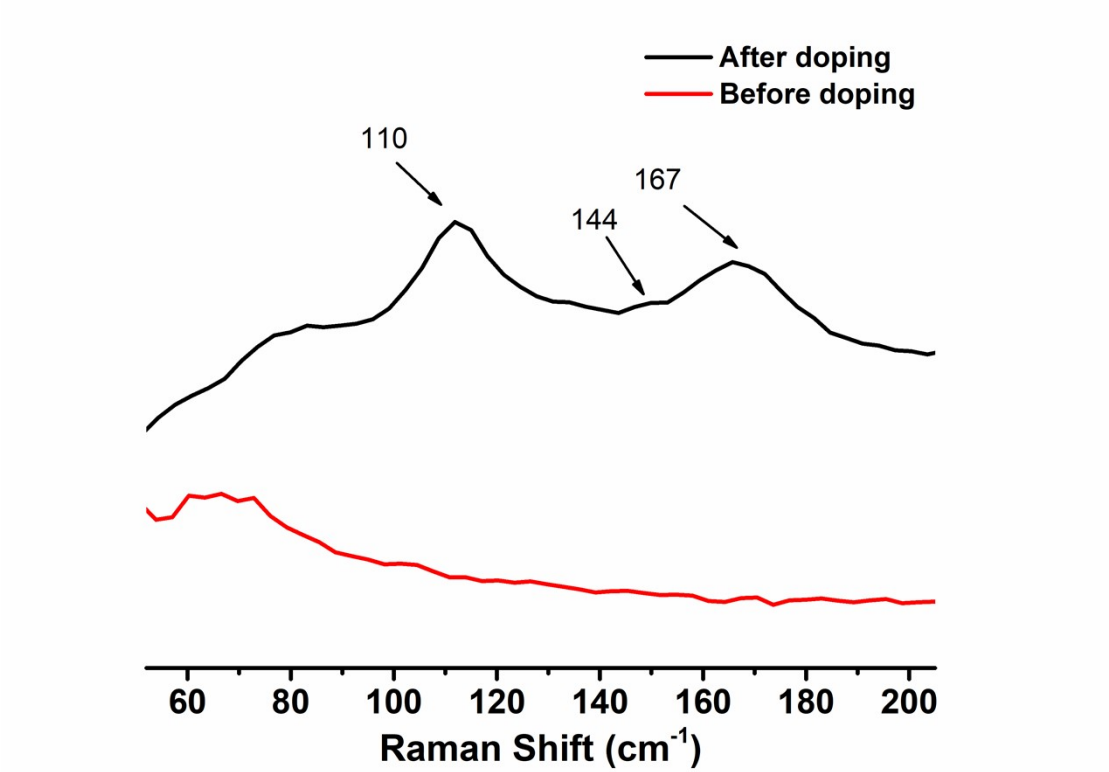

Figure S8. Raman spectra of AnPD-COF and I_2-doped AnPD-COF. After iodine doping, the newly emerging peaks appeared at 110, 144, and 167 cm^{-1}, which can be assigned to the perturbed iodine molecules, anionic I_3^-, and I_5^- species, respectively.

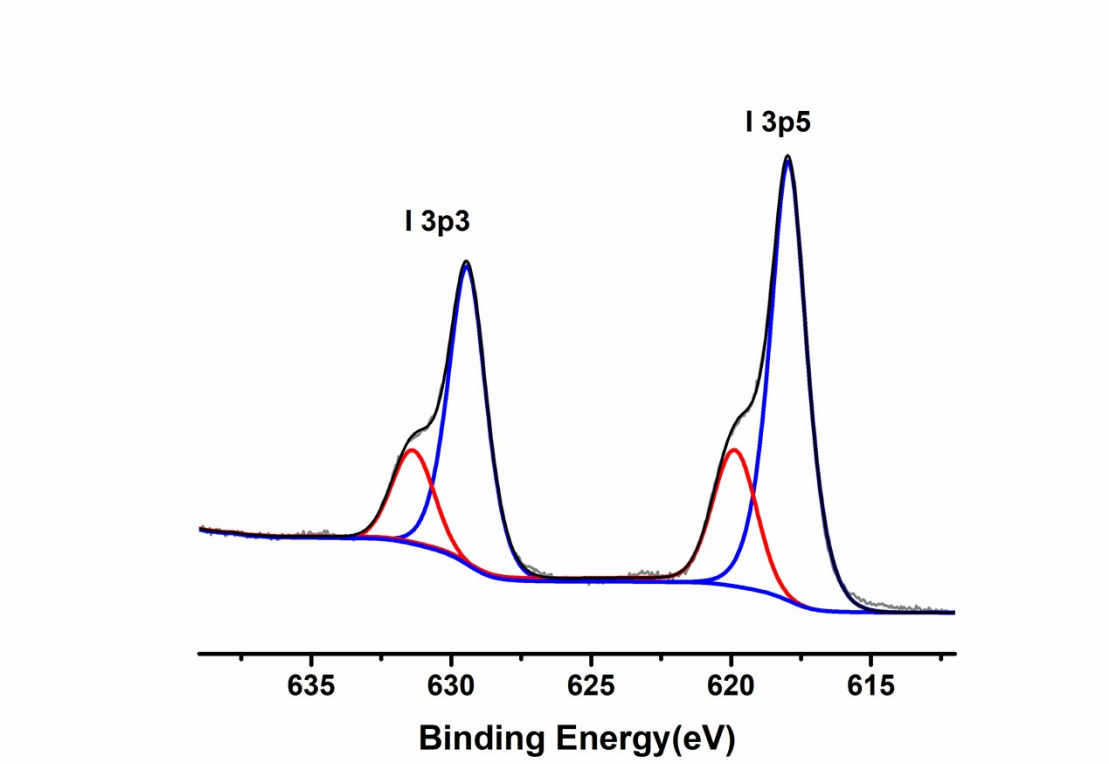

Figure S9. I 3p XPS spectrum of I_2-doped AnPD-COF. The two peaks of I 3p3 and I 3p5 can be deconvolved into two single peaks, respectively, of which the two peaks marked with blue correspond to the anionic species and the other two marked with red are attributed to the surface iodine adatoms.

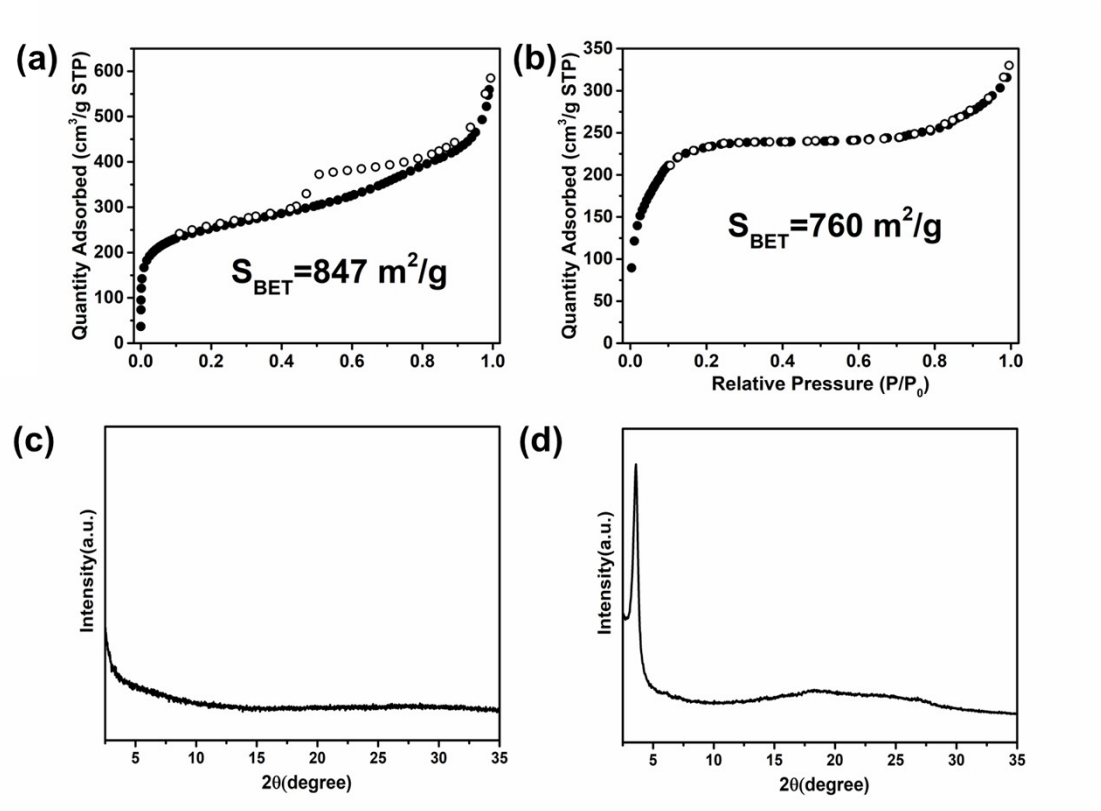

Figure S10. N_2 sorption isotherms and PXRD patterns of Poly-AnPD (a,c) and TFB-Bp-COF(b,d).

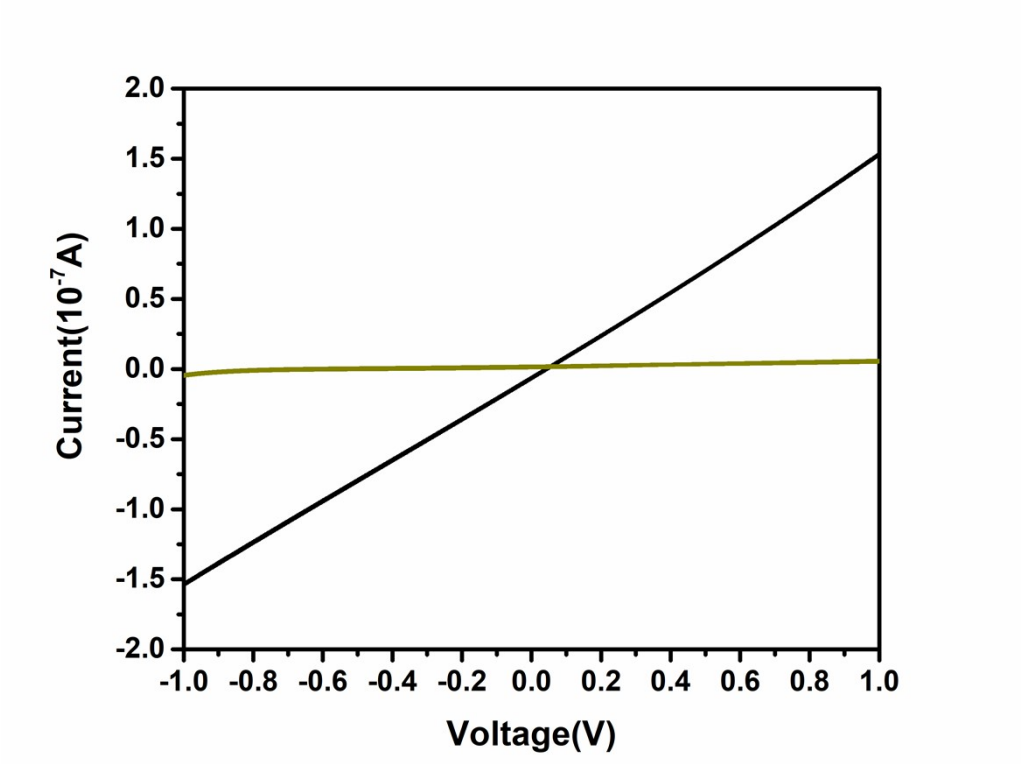

Figure S11. I-V curves of Poly-AnPD before and after doping. Yellow: before doping. Black: after doping.

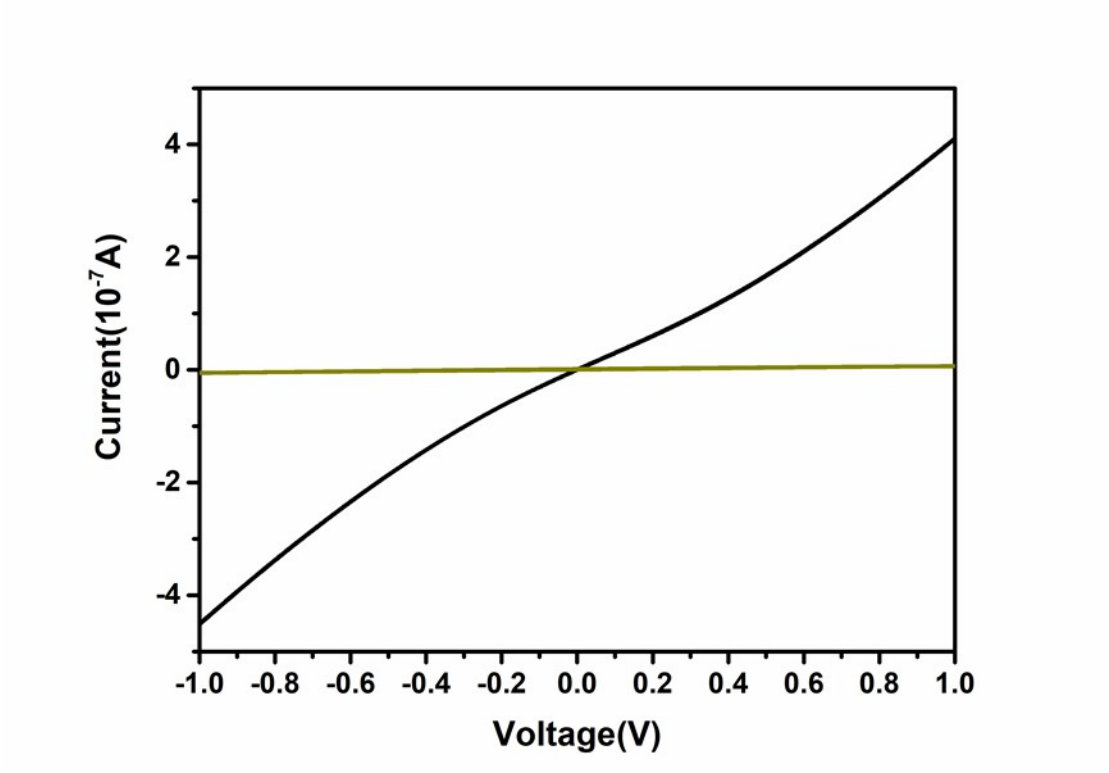

Figure S12. I-V curves of TFB-Bp-COF before and after doping. Yellow: before doping. Black: after doping.

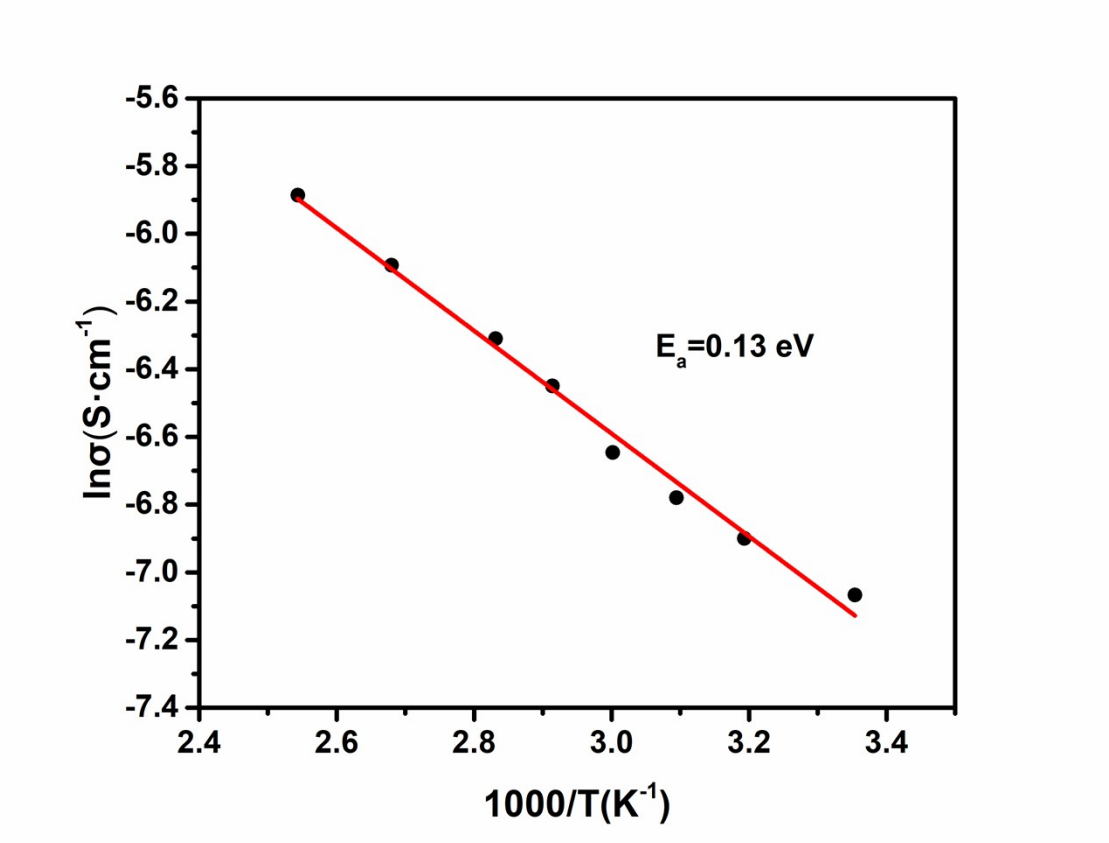

Figure S13. Arrhenius plot of conductivity vs. temperature for I_2-doped AnPD-COF. The activation energy was calculated to be 0.13 eV.

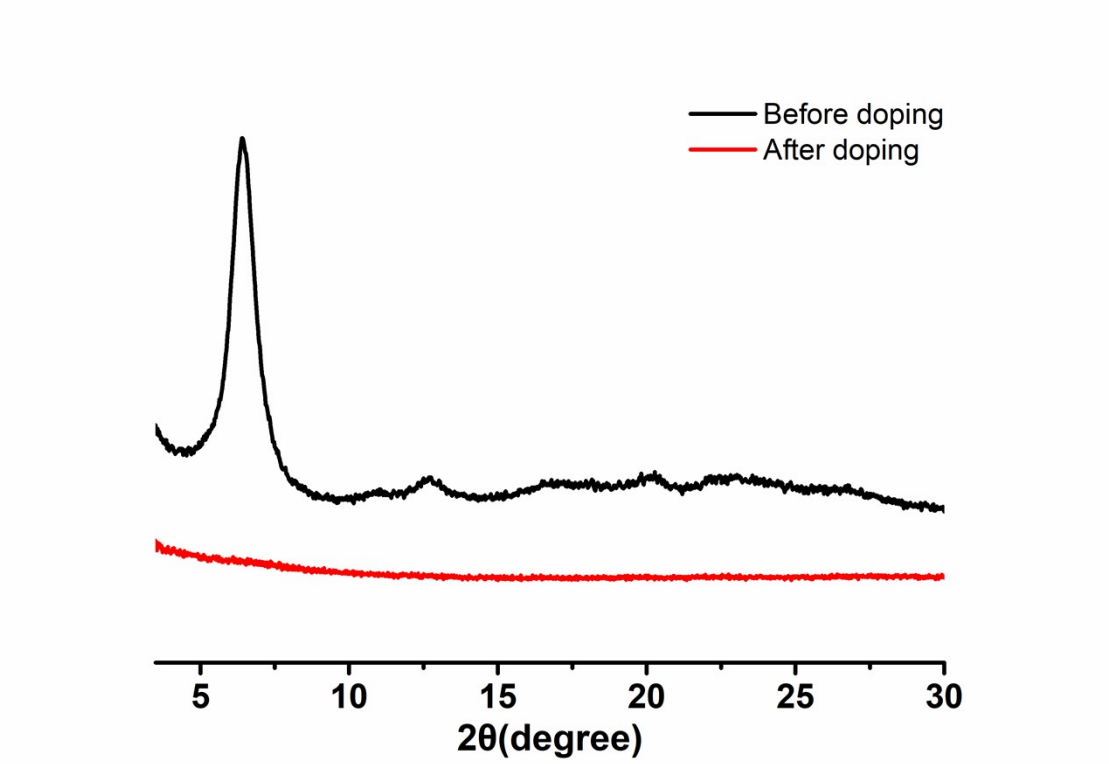

Figure S15. PXRD pattern comparison of AnPD-COF before and after iodine doping.

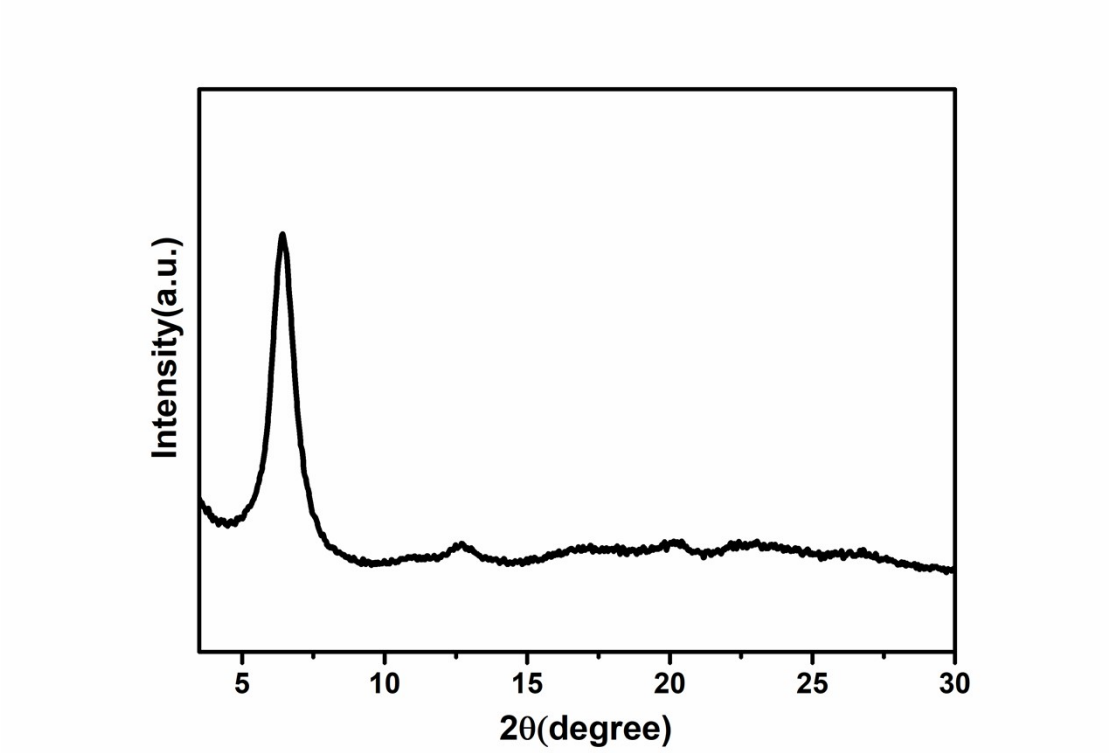

Figure S16. PXRD pattern of the remaining AnPD-COF after removal of the doped iodine.

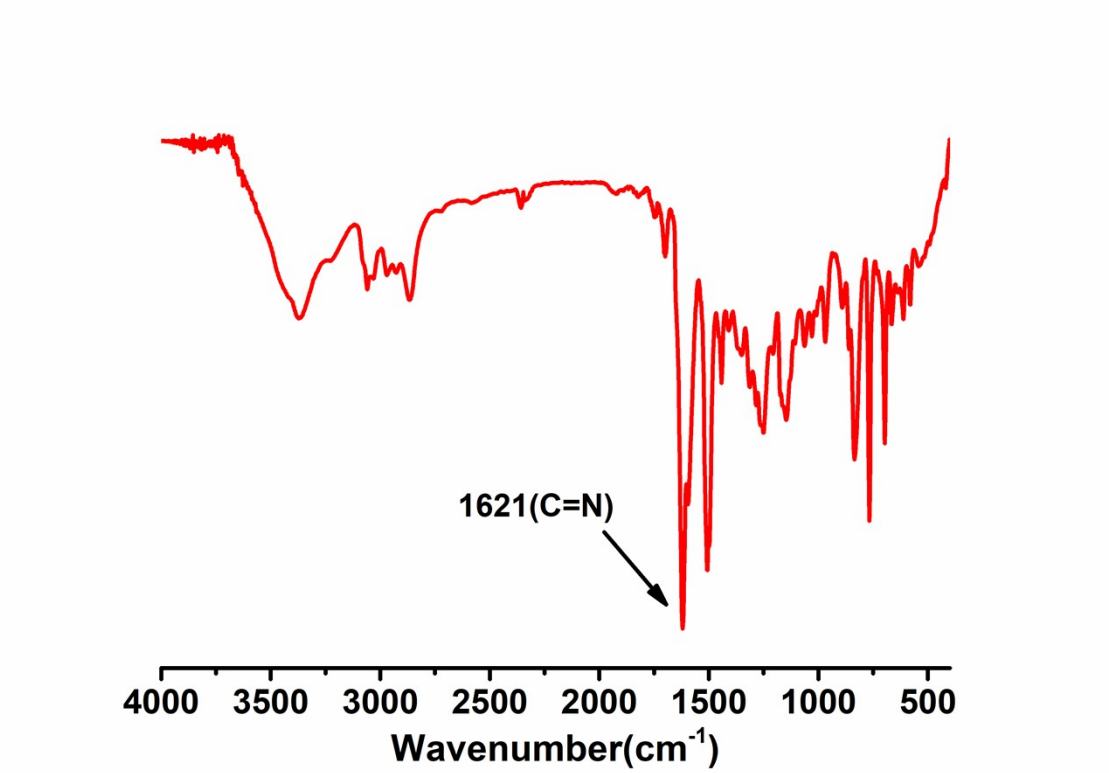

Figure S17. FT-IR spectrum of the remaining AnPD-COF after removal of the doped iodine.

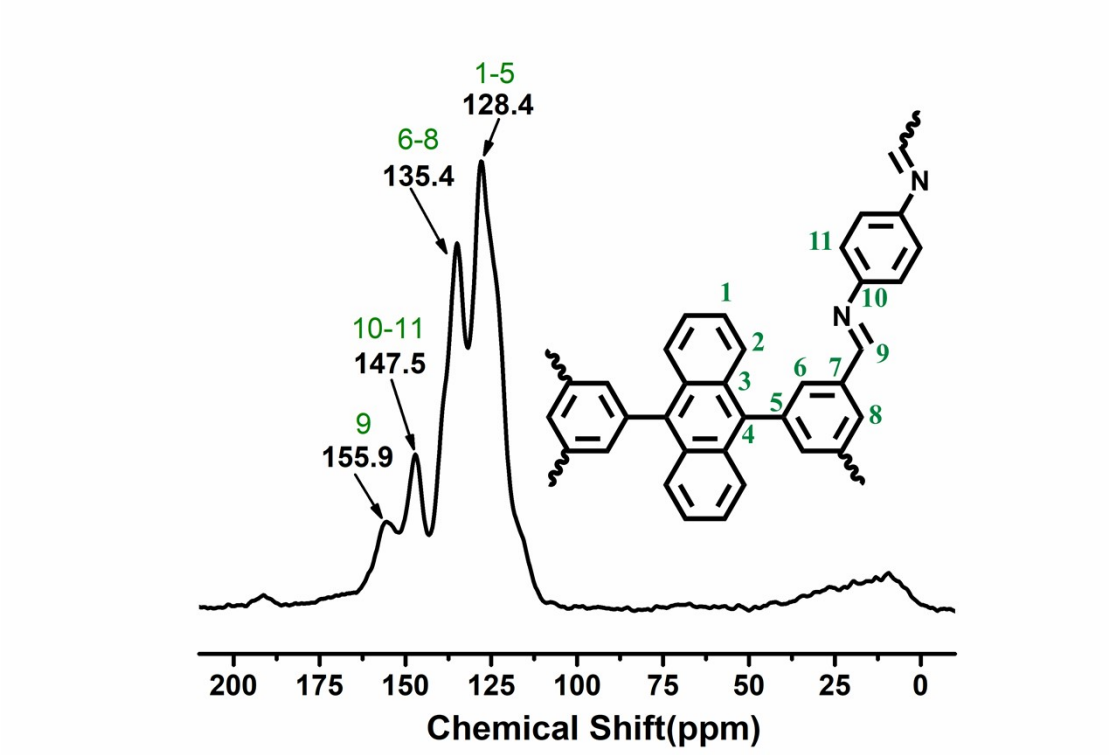

Figure S18. Solid-state CP/MAS ^{13}C NMR spectrum of the remaining AnPD-COF after removal of the doped iodine.

Table S1. Elemental analysis (EA) of AnPD-COF.

	C (wt%)	H (wt%)	N (wt%)	C/N molar ratio
EA	77.79	5.19	8.03	11.30
calculated	85.98	4.47	9.55	10.50

Table S2. Fractional atomic coordinates of the unit cell for AnPD-COF.

AnPD-COF:
AA stacking
Space Group: P1
a = 18.89016 ± 0.15944 Å, b = 16.94669 ± 0.14445 Å, c = 5.97109 ± 0.05087 Å
α = 127.24326 ± 0.02087°, β = 61.46254 ± 0.02874°, γ = 78.97743 ± 0.02660°

atom	x	y	z
C1	-0.565046599	0.47674517	0.575512374
C2	-0.477710276	0.415924976	0.122993692
C3	-0.41057279	0.43710284	0.046524841
C4	-0.432129105	0.520311322	0.424672761
C5	-0.51946427	0.581102423	0.877056181
C6	-0.586590966	0.559946102	0.953570973
C7	-0.671544017	0.623020103	1.414194957
C8	-0.680808988	0.685646331	1.764735396
C9	-0.615075876	0.705588194	1.689274795
C10	-0.542605055	0.661970798	1.265007447
C11	-0.325630896	0.374012556	-0.414141439
C12	-0.316345952	0.311377099	-0.764706624
C13	-0.382097456	0.291439593	-0.689188517
C14	-0.454549208	0.335067467	-0.264959882
C15	-0.627657536	0.445355268	0.629526387
C16	-0.369493569	0.551681343	0.370533953
C17	-0.604428968	0.360438377	0.620070742
C18	-0.650312512	0.31565658	0.5986436
C19	-0.719212569	0.355457981	0.578234654
C20	-0.746410053	0.443430359	0.599759434
C21	-0.701281735	0.487822328	0.631536791
C22	-0.295882323	0.509226056	0.368566163
C23	-0.250726125	0.553577505	0.40017365
C24	-0.277905109	0.64152668	0.421600482
C25	-0.346832376	0.681363638	0.401279824
C26	-0.392728926	0.636586794	0.379961453
C27	-0.819982704	0.486276075	0.586288524
N28	-0.863788671	0.44705471	0.581114307
C29	-0.623293818	0.225135841	0.576670546
N30	-0.559379466	0.183819615	0.596014487
C31	-0.373831241	0.771857928	0.423204466
N32	-0.437753755	0.8131965	0.403923598
C33	-0.177142102	0.510733664	0.413646138
N34	-0.13332802	0.549943657	0.418689758
C35	-0.932662015	0.479706092	0.555216535

C36	-0.53354828	0.094188044	0.558252329
C37	-0.064451727	0.517296553	0.444561543
C38	-0.463572858	0.90281556	0.441661747
C39	-0.973110324	0.565111465	0.568658835
C40	-0.961285576	0.415618351	0.493317228
C41	-0.558717002	0.029155128	0.426672214
C42	-0.47309153	0.061401617	0.629948048
C43	-0.438400191	0.967852562	0.573244548
C44	-0.524038975	0.935599058	0.369933895
C45	-0.023996229	0.431883077	0.431106906
C46	-0.035823185	0.581387871	0.506454026
H47	-0.728559322	0.618833864	1.477856822
H48	-0.740779785	0.723838409	2.105459109
H49	-0.625038157	0.75863318	1.972038941
H50	-0.5007278	0.688046901	1.213014772
H51	-0.268596476	0.378202811	-0.477801788
H52	-0.256390626	0.273193447	-1.105345186
H53	-0.372121704	0.238397099	-0.971915168
H54	-0.496439957	0.308988656	-0.212899632
H55	-0.545815103	0.320926873	0.60010669
H56	-0.754912336	0.322202054	0.556445645
H57	-0.720623507	0.552759239	0.635161211
H58	-0.276548917	0.444295707	0.365037287
H59	-0.24218514	0.674782765	0.44329607
H60	-0.451333652	0.676102019	0.399963595
H61	-0.833275065	0.54865126	0.569719421
H62	-0.667430597	0.201722478	0.583457801
H63	-0.329677102	0.79525789	0.41631614
H64	-0.163874919	0.448393836	0.430327794
H65	-0.955682318	0.618541897	0.628777767
H66	-0.930856784	0.352033729	0.493877079
H67	-0.607811725	0.053347437	0.382111051
H68	-0.448066954	0.106149338	0.700607805
H69	-0.389317417	0.943659409	0.617769193
H70	-0.549053255	0.89085748	0.299273171
H71	-0.041425637	0.378462956	0.371000974
H72	-0.066251337	0.644964106	0.505888349

Table S3. Comparison of activation energy (E_a).

COFs	Dopant	E_a (eV)	Ref.
AnPD-COF	Iodine	0.13	This work
ZnPc-pz COF	-	0.32	Ref. [S6]
CuPc-pz COF	-	0.37	Ref. [S6]
ZnPc-pz COF	Iodine	0.21	Ref. [S7]
TANG-COF	Iodine	<0.01	Ref. [S8]
JUC-518	Iodine	0.42	Ref. [S9]
JUC-519	Iodine	0.20	Ref. [S9]
NiPc-CoTAA	-	0.33	Ref. [S10]

Table S4. The comparison of carrier mobility values of different COFs.

COFs	Dopant	Method[a]	Hole Mobility ($cm^2 V^{-1} s^{-1}$)	Electron Mobility ($cm^2 V^{-1} s^{-1}$)	Ref.
AnPD-COF	Iodine	Hall effect	10.5	-	This work
AnPD-COF	-	Hall effect	0.7	-	This work
ZnPc-pz COF	Iodine	Hall effect	22	-	Ref. [S7]
ZnPc-pz COF	-	Hall effect	4.8	-	Ref. [S6]
CuPc-pz COF	Iodine	Hall effect	7	-	Ref. [S7]
CuPc-pz COF	-	Hall effect	0.9	-	Ref. [S7]
BUCT-COF-4	Iodine	Hall effect	-	2.62	Ref. [S11]
BUCT-COF-4	-	Hall effect	-	1.97	Ref. [S11]
TTF-Ph-COF	-	FP-TRMC	0.2	-	Ref. [S12]
TTF-Py-COF	-	FP-TRMC	0.08	-	Ref. [S12]
COF-366	-	FP-TRMC	8.1	-	Ref. [S13]
COF-66	-	FP-TRMC	3.0	-	Ref. [S13]
CS-COF	-	FP-TRMC	4.2	-	Ref. [S14]
H_2P-COF	-	FP-TRMC	3.5	-	Ref. [S15]
ZnP-COF	-	FP-TRMC	0.032	0.016	Ref. [S15]
CuP-COF	-	FP-TRMC	-	0.19	Ref. [S15]
NiPc COF	-	FP-TRMC	1.3	-	Ref. [S16]
HBC-COF	-	FP-TRMC	0.7	-	Ref. [S17]
2D-NiPc-BTDA COF	-	FP-TRMC	-	0.6	Ref. [S18]
2D D-A COF	-	FP-TRMC	0.01	0.04	Ref. [S19]

[a]Hall effect method and flash-photolysis time-resolved microwave conductivity (FP-TRMC)

Table S5. The comparison of the BET surface area of AnPD-COF, Poly-AnPD, and TFB-Bp-COF.

Sample	$S_{BET}(m^2\ g^{-1})$
AnPD-COF	725
Poly-AnPD	847
TFB-Bp-COF	760

Table S6. The comparison of the doped iodine contents in the different samples.

sample	weight (wt%)
AnPD-COF	140.4
Poly-AnPD	144.1
TFB-Bp-COF	143.5

Table S7. Calculations of IPs for the various models.

Model	Neutral(hatree)	Cation(hatree)	IP(hatree)	IP(eV)
Dp	-463.261715	-462.956608	0.305107	8.30
Dp-dimer	-926.528676	-926.250958	0.277718	7.56
Ant	-1001.549833	-1001.293022	0.256811	6.99
Ant-dimer	-2003.083083	-2002.849642	0.233441	6.35

Reference

[S1] Q. Gao, L. Bai, Y. Zeng, P. Wang, X. Zhang, R. Zou and Y. Zhao, *Chem. Eur. J.*, 2015, **21**, 16818-16822.

[S2] M. J. Frisch, G. W. Trucks, H. B. Schlegel, G. E. Scuseria, M. A. Robb, J. R. Cheeseman, G. Scalmani, V. Barone, G. A. Petersson, H. Nakatsuji, X. Li, M. Caricato, A. V. Marenich, J. Bloino, B. G. Janesko, R. Gomperts, B. Mennucci, H. P. Hratchian, J. V. Ortiz, A. F. Izmaylov, J. L. Sonnenberg, D. Williams-Young, F. Ding, F. Lipparini, F. Egidi, J. Goings, B. Peng, A. Petrone, T. Henderson, D. Ranasinghe, V. G. Zakrzewski, J. Gao, N. Rega, G. Zheng, W. Liang, M. Hada, M. Ehara, K. Toyota, R. Fukuda, J. Hasegawa, M. Ishida, T. Nakajima, Y. Honda, O. Kitao, H. Nakai, T. Vreven, K. Throssell, J. A. Montgomery, Jr., J. E. Peralta, F. Ogliaro, M. J. Bearpark, J. J. Heyd, E. N. Brothers, K. N. Kudin, V. N. Staroverov, T. A. Keith, R. Kobayashi, J. Normand, K. Raghavachari, A. P. Rendell, J. C. Burant, S. S. Iyengar, J. Tomasi, M. Cossi, J. M. Millam, M. Klene, C. Adamo, R. Cammi, J. W. Ochterski, R. L. Martin, K. Morokuma, O. Farkas, J. B. Foresman, and D. J. Fox, Gaussian16, Revision A.03, Gaussian, Inc.:Wallingford CT, 2016.

[S3] Zhao, Y.; Truhlar, D. G., Theor. Chem. Acc., 2008, 120, 215; Florian Weigend and Reinhart Ahlrichs, *Phys. Chem. Chem. Phys.*, 2005, 7, 3297-3305.

[S4] S. Grimme, S. Ehrlich, L. Goerigk, *J. Comput. Chem.*, 2011, **32**, 1456-1465.

[S5] T. Vikramaditya and S. T. Lin, *J. Comput. Chem.*, 2017, **38**, 1844-1852.

[S6] M. Wang, M. Ballabio, M. Wang, H. H. Lin, B. P. Biswal, X. Han, S. Paasch, E. Brunner, P. Liu, M. Chen, M. Bonn, T. Heine, S. Zhou, E. Canovas, R. Dong and X. Feng, *J. Am. Chem. Soc.*, 2019, **141**, 16810-16816.

[S7] M. Wang, M. Wang, H. H. Lin, M. Ballabio, H. Zhong, M. Bonn, S. Zhou, T. Heine, E. Canovas, R. Dong and X. Feng, *J. Am. Chem. Soc.*, 2020, **142**, 21622-21627.

[S8] V. Lakshmi, C. H. Liu, M. Rajeswara Rao, Y. Chen, Y. Fang, A. Dadvand, E. Hamzehpoor, Y. Sakai-Otsuka, R. S. Stein and D. F. Perepichka, *J. Am. Chem. Soc.*, 2020, **142**, 2155-2160.

[S9] H. Li, J. Chang, S. Li, X. Guan, D. Li, C. Li, L. Tang, M. Xue, Y. Yan, V. Valtchev, S. Qiu and Q. Fang, *J. Am. Chem. Soc.*, 2019, **141**, 13324-13329.

[S10] Y. Yue, P. Cai, X. Xu, H. Li, H. Chen, H. C. Zhou and N. Huang, *Angew. Chem. Int. Ed.*, 2021, **60**, 10806-10813.

[S11] S. Wang, X. X. Li, L. Da, Y. Wang, Z. Xiang, W. Wang, Y. B. Zhang and D. Cao, *J. Am. Chem. Soc.*, 2021, **143**, 15562-15566.

[S12] S. Jin, T. Sakurai, T. Kowalczyk, S. Dalapati, F. Xu, H. Wei, X. Chen, J. Gao, S. Seki, S. Irle and D. Jiang, *Chem. Eur. J.*, 2014, **20**, 14608-14613.

[S13] S. Wan, F. Gándara, A. Asano, H. Furukawa, A. Saeki, S. K. Dey, L. Liao, M. W. Ambrogio, Y. Y. Botros, X. Duan, S. Seki, J. F. Stoddart and O. M. Yaghi, *Chem. Mater.*, 2011, **23**, 4094-4097.

[S14] J. Guo, Y. Xu, S. Jin, L. Chen, T. Kaji, Y. Honsho, M. A. Addicoat, J. Kim, A. Saeki, H. Ihee, S. Seki, S. Irle, M. Hiramoto, J. Gao and D. Jiang, *Nat. Commun.*, 2013, **4**, 2736.

[S15] X. Feng, L. Liu, Y. Honsho, A. Saeki, S. Seki, S. Irle, Y. Dong, A. Nagai and D. Jiang, *Angew. Chem. Int. Ed.*, 2012, **51**, 2618-2622.

[S16] X. Ding, J. Guo, X. Feng, Y. Honsho, J. Guo, S. Seki, P. Maitarad, A. Saeki, S. Nagase and D. Jiang, *Angew. Chem. Int. Ed.*, 2011, **50**, 1289-1293.

[S17] S. Dalapati, M. Addicoat, S. Jin, T. Sakurai, J. Gao, H. Xu, S. Irle, S. Seki and D. Jiang, *Nat. Commun.*, 2015, **6**, 7786.

[S18] X. Ding, L. Chen, Y. Honsho, X. Feng, O. Saengsawang, J. Guo, A. Saeki, S. Seki, S. Irle, S. Nagase, V. Parasuk and D. Jiang, *J. Am. Chem. Soc.*, 2011, **133**, 14510-14513.

[S19] X. Feng, L. Chen, Y. Honsho, O. Saengsawang, L. Liu, L. Wang, A. Saeki, S. Irle, S. Seki, Y. Dong and D. Jiang, *Adv. Mater.*, 2012, **24**, 3026-3031.